

Water Absorption Effect on the Dynamic Properties of Nylon-6 by Dielectric Spectroscopy

E. Laredo,^{*,†} M. Grima,[‡] F. Sánchez,[†] and A. Bello[†]

Physics Department and Materials Science Department, Universidad Simón Bolívar, Apartado 89000, Caracas 1080, Venezuela

Received July 7, 2003; Revised Manuscript Received September 23, 2003

ABSTRACT: New results of dielectric spectroscopy in semicrystalline nylon-6 samples with different moisture contents are presented by using a wide frequency (10^{-2} – 3×10^6 Hz) and temperature range (133–433 K). The dielectric absorption spectra in frequency domain are decomposed in Cole–Cole distributions corresponding to the local γ and β modes, two segmental α modes, and a high-intensity Maxwell–Wagner–Sillars relaxation. The presence of two segmental relaxations in the isothermal runs, attributed to the plasticized and the unplasticized α mode, is interpreted as the manifestation of two different length and time scales of cooperative motions. A quantitative comparison between the results obtained for the wet and dry samples, such as relaxation times variation, activation energies, Vogel–Tammann–Fulcher parameters, dielectric increments, and distribution widths, is presented for each mode and shows how the progressive drying of the sample during the experiment affects all these quantities.

Introduction

Polyamides with variable chain lengths form a family of engineering resins which dynamics have been extensively studied by mechanical and dielectric techniques. The intra- and interchain hydrogen bonds play an important role in the formation of crystalline lamellae and in the relaxation mechanisms occurring when water molecules enter the material. The H bonds between two neighboring amide groups can be modified by moisture sorption and results in important changes in the mobility of molecular entities either local or segmental. Recent studies on dry and wet samples of nylon-6 by thermally stimulated depolarization currents (TSDC) have shown with this sensitive technique the effect of humidity on the low-temperature,¹ γ and β , and high-temperature, α , relaxations.² According to Puffr and Sebenda,³ the moisture absorption may result in different states for the water molecules. They can be either tightly bound to the carbonyl groups, creating double H bonds between neighboring CO groups, or weakly bound to existing H bonds, or in larger aggregates if several water molecules cluster together. Also, the presence of freezable free water in existing cavities could be possible at high water contents.¹ Dynamic mechanical analysis (DMA) has been widely used to follow the mechanical relaxations in nylons^{4–7} and the influence of moisture on the H bonds existing in these materials. A compilation of the early works is summarized in McCrum et al.⁸ When comparing dielectric spectra given by nylons with various lengths of the methylenic sequence, one observes that odd nylons give markedly higher intensities than the even ones for the main relaxation mode.⁹ The orientation and the degree of crystallinity of the sample also affect the intensity of the α mode as has been shown in nylon-6,¹⁰ At high water concentrations, h , the β relaxation becomes predominant as the γ peak intensity decreases. As the drying process advances, the γ relaxation intensity

increases and the β one slowly diminishes. The plasticization effect is very important in nylon-6 and evidenced by the significant shift to lower temperatures of the α relaxation which is the dielectric² or mechanical manifestation of the onset of the cooperative motions which take place at the glass–rubber transition temperature, T_g , of the polymer. In nylon-12 the plasticization effect of water is also observed as a shift to lower temperatures in the mechanical dynamic glass transition, the shift being of ca. 20 K^5 as compared to nylon-6 where the α peak as observed by TSDC shifts ca. 90 K^2 . Additionally, a dielectric relaxation mode located at temperatures higher than T_g has been observed in nylon-12 by Pathmanathan and Johari.¹¹ Boyd¹² in a review of the relaxation processes in crystalline polymers does not find in the polyamides a crystal-related relaxation mode that he labeled as the α mode and that in this work will be called α_c mode to avoid confusions with the glass transition relaxation. This absence is justified by the existence of a high misfit energy due to the crystalline structure of the polyamides which renders difficult these kinds of motions.

The experimental works on polyamides with dielectric spectroscopy (DS) are numerous, and the results agree with the DMA on the dependence of the intensity and position of the low-temperature relaxations as the humidity level, h , increases.^{13,14} As to the determination of the relaxation parameters in Ny-6, the quantitative analysis of the spectrum is rendered complicated in frequency domain as the frequency range often used in early pioneer works⁸ is not wide enough to analyze precisely the details of the relaxations characteristic of these resins.

The aim of the present work is to present experimental dielectric spectroscopy (DS) results on nylon-6 films which show features that have not been reported before on this important polymer and which are explained by the changes occurring in the material as the experiment progresses. Also, detailed analysis of the relaxation spectra will allow to draw relaxation plots which leads to the precise determination of the relaxation parameters and evidence the presence of relaxation modes

[†] Physics Department.

[‡] Materials Science Department.

* Corresponding author: e-mail elaredo@usb.ve.

which give precious indications about the drying process.

Experimental Results and Analysis

Samples of nylon-6, 21 μm thick and 20 mm in diameter, were cut from compression-molded films. The pellets are from Akzo Chemicals, with a density of 1.13 g/cm³, and the crystallinity degree of the films used here as determined by wide-angle X-ray scattering is 67%.

The DS experiments measuring the complex dielectric constant $\epsilon^* = \epsilon' - i\epsilon''$ were performed in a Novocontrol Concept Twelve spectrometer with frequencies ranging from 10⁻² Hz to 3 MHz. The system is based on a Schlumberger frequency response analyzer (FRA SI 1260) with a dielectric converter and a temperature controller which provides a stability of better than 0.1 K by means of a cold nitrogen flux. The sample is located between two horizontal metallic electrodes, and a permanent gaseous dry nitrogen flux is the exchange gas. Before all experiments the samples were immersed in distilled water for 24 h at room temperature, and then their surface was dried before placing them in the measuring dielectric cell. In our previous work on Ny-6 the amount of water concentration in weight, h , absorbed after a similar hydration procedure was estimated to be of 10%. As the TSDC equivalent frequency is in the range of millihertz, the dielectric manifestation of the glass transition of the plasticized material occurs below room temperature, and no significant changes in h are expected. In the present DS experiments where the frequency range reaches 3 MHz the α mode shifts to higher temperatures as the frequency increases, and its observation implies a progressive reduction in the water content of the sample. This variation in the water content as the temperature increases results in changes in the material from one isothermal to the next until the hydration level in the experimental conditions does not change anymore.

The experiments (A) were carried from 133 to 428 K by 5 K steps. At each temperature the chosen 35 frequencies (0.01 Hz < ν < 3.16 MHz) were measured, which implies a plateau 17 min long at each temperature value up to the final temperature; this is equivalent to a 0.21 K/min ramp. These measurements are referred as the A runs on wet samples. After reaching the final temperature the program is reversed, and the sample is taken back to 133 K.

A second set of experiments (B) was performed with a much faster temperature ramp, 1.95 K/min, with only two measuring frequencies 100 and 1000 Hz, to compare the effects of slow and fast temperature ramps on the dielectric results. These experimental protocols are quite different from that used in the TSDC experiments reported in a previous work,² where the wet sample was polarized at increasing temperatures as the moisture content of the sample decreased, and the polarization temperature was chosen so as to activate the relaxation modes up to the segmental one only.

The analysis of the dielectric spectra was carried out by decomposing the experimental trace of the imaginary part of the dielectric constant as a function of the angular frequency, $\epsilon''(\omega)$, recorded at different temperatures into up to three relaxation modes each with a Cole–Cole distribution of relaxation time. This symmetric distribution function is chosen on the basis of our experience in fitting relaxation modes in semicrystalline polymers,^{15,16} which agrees with Boyd's¹² observations. The contribution of the conductivity is added and taken as proportional to ω^{-1} . For each mode the complex dielectric constant, ϵ^* , is given by

$$\epsilon^*(\omega, T) = \epsilon_\infty + \frac{\epsilon_s - \epsilon_\infty}{1 + (i\omega\bar{\tau}(T))^\alpha} \quad (1)$$

where ϵ_∞ is the high-frequency value of the dielectric constant, ϵ_s is its static value, $\bar{\tau}(T)$ is the relaxation time mean value of the symmetric Cole–Cole distribution at a given temperature T , and α is a parameter which characterizes the distribution width and which is equal to 1 for a Debye process. The

experimental trace recorded at constant temperature is thus fitted to the following expression

$$\epsilon''(\omega) = \sum_{k=1}^3 \frac{\Delta\epsilon_k (\omega\bar{\tau}_k)^{\alpha_k} \sin(\pi\alpha_k/2)}{1 + 2(\omega\bar{\tau}_k)^{\alpha_k} \cos(\pi\alpha_k/2) + (\omega\bar{\tau}_k)^{2\alpha_k}} - \frac{\sigma_0}{\epsilon_0\omega} \quad (2)$$

where ϵ_0 denotes the permittivity of free space and with $\Delta\epsilon_k = (\epsilon_s - \epsilon_\infty)_k$ being the dielectric strength for the k th mode. At each temperature a value of $\bar{\tau}_k(T)$ is found for the modes present in the frequency window used here. The relaxation diagrams are plots representing the variation of $\log \bar{\tau}_k(1/T)$, which is expected to be linear in the case of Arrhenius dependences for the relaxation time and curved for Vogel–Tammann–Fulcher (VTF) ones, according to the following expressions:

$$\tau(T) = \tau_0 \exp[E_A/kT], \quad \tau_{\text{VTF}}(T) = \tau'_0 \exp[E_{\text{VTF}}/k(T - T_0)] \quad (3)$$

τ_0 and τ'_0 are the preexponential factors; E_A and E_{VTF} are the characteristic energy for the Arrhenius and VTF relaxation times, respectively.

The fitting procedure is complicated because of the presence of very often incomplete peaks despite the extension of the frequency window of more than 8 decades. As the temperature increases, the relaxation peaks shift to higher frequencies and sweep the frequency window with different speeds characteristic of the relaxation energy of each mode. The fittings are performed with the nonlinear least-squares standard procedure (WINFIT from NOVOCONTROL) starting from different initial parameters. Each of the isotherm runs was fitted independently, and the final results were accepted if the final parameters presented a smooth variation in a wide temperature range.

Results and Discussion

The results obtained on the wet and dry samples following the temperature program A in order to take advantage of the wide frequency range available in our DS system are presented in the following sections. The results obtained with program B where the wet and dry materials are studied only at two frequencies and with a temperature ramp sufficiently fast to minimize significant changes in the material during the measurement will also be presented.

Comparison of the DS Spectra for the Wet and Dry Samples. The results for the first series of experiments of $\epsilon'(T)$ and $\epsilon''(T)$ were carried out from 133 to 428 K and then back to 133 K, by starting with a water-saturated sample. During the heating run, the nylon-6 sample in the wet state is progressively dried, and the subsequent cooling experiment is made on a dry sample of nylon-6. The results for $\log(\epsilon''(T))$ and $\epsilon'(T)$, for $\nu = 1000$ Hz, are plotted in Figure 1a,b with symbols joined by lines for the heating runs and continuous and interrupted lines only for the cooling ones. These plots as a function of temperature are very useful to identify visually the existing relaxation modes, but because of their width, it is difficult to discard the existence of processes, which might be overlapping the most intense ones. The precise quantitative analysis in frequency domain will give the final insight into that question. It is to be noted that the experimental trace intensity in both $\epsilon''(T)$ and $\epsilon'(T)$ is lower than absolute values found in the literature for other aliphatic polyamides.^{5,7,9,10} Several possibilities may be considered to account for these low values. First, the sample presents a high crystallinity, as determined by WAXS, caused by small crystallites distributed throughout the sample. The

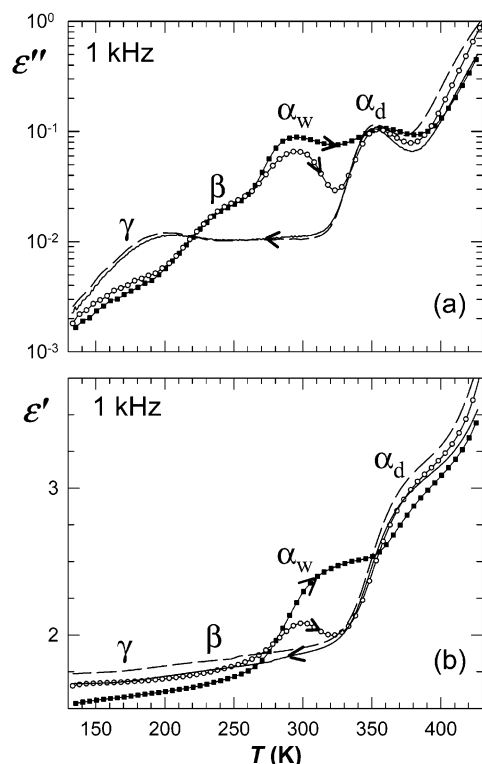


Figure 1. Variation of (a) $\log(\epsilon''(T))$ and (b) $\epsilon'(T)$ at 1 kHz for the wet sample (\circ , temperature program A; \blacksquare , temperature program B) and for the dry sample ($- -$, temperature program A; $-$, temperature program B). The arrows indicate the direction of the temperature variation for each curve.

restrictions imposed by these ordered zones on the adjacent amorphous regions could additionally decrease the amount of orientable dipoles. Second, the experimental trace is the result of overlapping peaks which separation and further merging at high frequency/or temperature depends on the specific dynamics of each material as it has been demonstrated in the amorphous polymethacrylate series.¹⁷

Important differences are noted between the four runs presented in Figure 1. The wet sample spectrum presents a more complicated structure than the dry sample one. The dry sample absorption spectra, independent of the rate at which the temperature is decreased, are very similar (continuous and interrupted lines). It is easily observed in Figure 1a that the temperature region below 273 K, made of two wide relaxations, γ and β , much weaker than the rest of the spectrum, presents an inversion in the relative intensities of these two modes on going from the wet to the dry sample. In the wet sample the γ mode is the weakest one with an intensity in the 10^{-3} range for the ϵ'' values. The β mode is more intense than the lowest temperature one. In the dry sample the γ mode intensity increases, in addition to a slight shift to higher temperatures, and the β mode is now the less intense of the two. These facts are in excellent agreement with the TSDC previous works^{1,2} where the variation of the position and intensity of these peaks with the humidity level has been thoroughly studied. The interpretation is based on the absorption scheme proposed by Puffr and Sebenda.³ In the wet sample, the tightly bound water molecules create double H bonds between neighboring carbonyl groups that in the dry material were bound to NH groups, thus decreasing the number of reorienting dipolar entities whose motion causes the γ process. The increase in T_M ,

as the sample is dried has been related to the possible increase in length of the $(CH_2)_n$ sequence accompanying the polar group motion. The β mode behavior has also been attributed to the firmly bound water which in this case increases the peak intensity, i.e., the number of reorienting dipoles or their dipolar moment. A possible origin is the water–amide complexes present in wet samples, in agreement with previous interpretations.^{1,18}

At higher temperatures, the peak at 293 K in Figure 1a, which is labeled here α_w , is intense in the wet sample and almost disappears in the dry sample. Additionally, it is less intense and better resolved in the experiment made with a slower ramp (program A), i.e., in the sample where the drying procedure is more advanced at temperatures where this peak occurs. This mode is the dielectric manifestation of the glass–rubber transition of Ny-6, which has been thoroughly studied by TSDC.² The variations observed in this mode as the drying procedure progresses are proof that the material is undergoing changes in the degree of plasticization with consequences in the chain mobility as the temperature increases. The α_w relaxation might be the result of the superposition of several segmental modes corresponding to different humidity contents.

The last peak in Figure 1a on the high-temperature side of the spectrum (α_d mode) is present in the four runs plotted here and is located at 353 K for the 1 kHz frequency; i.e., it is nearly independent of the thermal treatment and therefore shows for the four runs a similar water concentration at these temperatures. One can note only very little differences, the α_d peak corresponding to the driest sample, i.e., the slowest temperature ramp (A), being slightly more intense than the other ones. It is to be noted that the α_d peak is narrower than the α_w one as the material at these high temperatures has released all the water molecules susceptible to leave the sample at this stage. The high-temperature rise in $\log(\epsilon''(T))$ observed in Figure 1a is attributed to the low-temperature tail of modes occurring at $T > T_g$ and to the onset of the conductivity of the sample which is very important in this material.

In Figure 1b, the comparison of the wet and dry sample shows an extra feature on the high-temperature tail of the α_w mode in the $\epsilon'(T)$ curve. The dielectric permittivity, $\epsilon'(T)$, of the wet sample for the slowest temperature ramp (program A, open symbols) shows a maximum around room temperature which is absent in the dry sample spectrum. The last part of the spectrum that corresponds to the α_d region in the loss diagram appears as a pronounced bump in a steep rise of the dielectric constant at high temperatures, present in both the wet and dry samples. The presence of a maximum in the $\epsilon'(T)$ trace will be confirmed below by studying a wider frequency range. This drop in the dielectric compliance of the wet sample is an indication of a major change in the material in this temperature interval, which corresponds to a mode detected in the loss spectrum shown in Figure 1a. The decrease in the $\epsilon'(T)$ trace is analogous to an increase in the rigidity of the sample as a result of the vitrification of the material due to the loss of moisture. The presence of another segmental mode at higher temperatures confirms the existence of a glass transition corresponding to the material that has been progressively dried. A similar $\epsilon'(T)$ behavior has been reported by Massalska-Arodz et al.^{19,20} in low molecular weight glass-forming liquids for cooling and heating experiments. In these materials

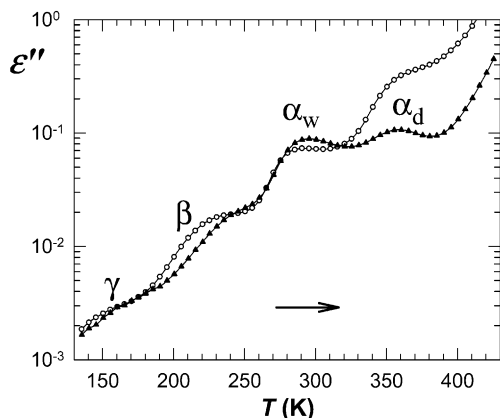


Figure 2. Variation of $\log(\epsilon''(T))$ for the wet nylon-6 sample at 1 kHz (▲) and 100 Hz (○) with temperature program B.

the decrease in $\epsilon'(T)$ is attributed to the replacement of a supercooled liquid by a rigid crystalline material. In the temperature range of our work no changes in the crystallinity of the material are expected and the fall in the dielectric constant is due to the decrease of the water plasticization effect. When the experiment is carried with a fast temperature ramp the wet sample also starts to lose moisture, but the drying procedure is not as efficient as in the run with the lowest rate for the temperature increase where the sample is kept at each temperature step an average time of 17 min. Because of the well-known plasticization effect of water molecules present in the wet sample, one expects that the glass transition temperature will be shifted to lower temperatures; a shift of ca. -86 K on going from a dry up to a 10% weight concentration of moisture in the wet sample has been reported in nylon-6 by TSDC.² The search for the origin of the modes present above 273 K in the wet sample is clarified by comparing the traces obtained on the wet sample at two different frequencies while the temperature of the sample is increased at a linear rate of 1.95 K/min, program B, which are presented in Figure 2.

One can observe that, as expected, the position of the peaks γ , β , α_w , and α_d are shifted to higher temperatures on going from 100 to 1000 Hz. However, the rise in the low-temperature tail of the α_w peak is common to both frequencies. In Figure 3a, where the results for $\epsilon''(T)$ for the wet sample obtained for a wide frequency range are plotted, this feature is clearly seen for frequencies from 10 kHz to 1 Hz. As the frequency is lowered, the high-temperature contributions become so huge that it affects the profile of the α_w peak and the collapse of the traces around 273 K is not that evident. This is indicative of the presence of a composite peak in this temperature region for the wet sample, one of the components being located at the same temperature even when the frequency changes by decades. This peak might be originated by the water molecules forming clusters in the material which undergo a phase transition in this confined environment. The decrease in intensity in the α_w region on going from the wet to the dry samples, shown in Figure 1a, is caused by the disappearance of the fixed frequency peak and a lesser contribution from the modes β and α_w attributed to the presence of water molecules in the sample.

The overlap of the two segmental processes is less pronounced in the sample heated slowly than in the sample heated with a faster temperature ramp. At 328 K the water level is not sufficient to plasticize the

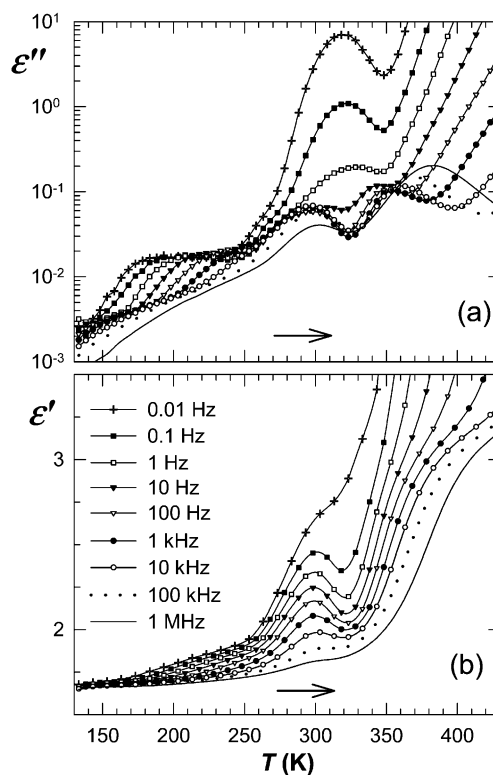


Figure 3. Variation of the imaginary (a) and real (b) part of the dielectric constant of the wet nylon-6 film for frequencies $0.01 \text{ Hz} \leq \nu \leq 1 \text{ MHz}$. Data taken during the heating run, temperature program A.

material and regions where the segmental mobility is reduced originate the α_d peak that appears at 353 K at 1 kHz. The similarity of the wet and dry samples spectra at high temperatures confirms the attribution of the α_d peak to the cooperative mode which corresponds to the glass transition temperature of the driest material reached with these experimental conditions. The changes observed in the wet and dry traces at lower temperatures and its explanation based on a combined effect of clusters of water molecules and the glass transition of the wet material are also sustained by the maximum observed in this temperature region in the $\epsilon'(T)$ curves presented in Figure 3b, which evidences the changes in the material.

Determination of the Relaxation Time Distribution for Each Mode in the Wet Sample. The analysis of the DS experiments is carried out in frequency domain on isothermal curves as described in the Experimental Section. In Figure 4, a sequence of the decomposition obtained for the wet sample at four increasing temperatures is presented. The fitting procedure is a difficult one owing to the number of relaxations present, to their incomplete contributions at high temperatures within the frequency window used in this work, and to the high-conductivity contribution at low frequencies and high temperatures, which overlaps the low-frequency tail of the peaks under study. Many attempts are made from different starting parameters until the best fit is obtained. Several new features, which could not be guessed by studying the isochrone spectra presented before, were found after this decomposition in Cole–Cole distributions. At low temperatures the wet sample is well described by the sum of the γ_w and β_w local processes, the first one being weaker than the β mode. In Figure 4a the decomposition

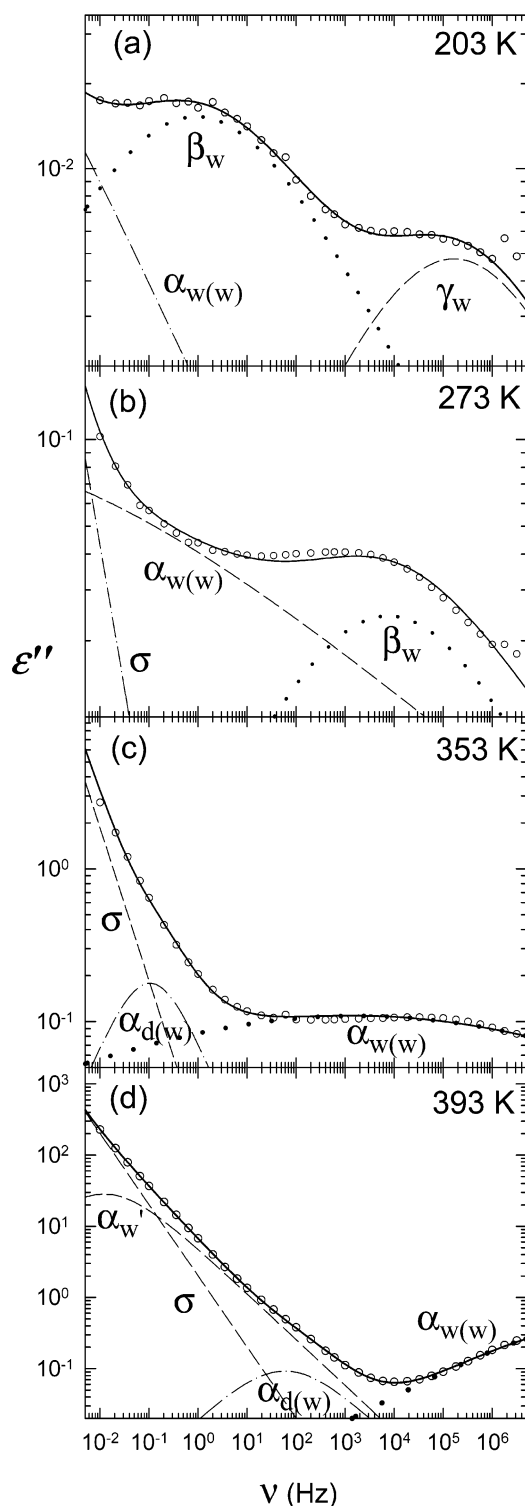


Figure 4. Decomposition in Cole–Cole distributions of the isothermal runs $\epsilon''(\nu)$ for the wet nylon-6 sample: (○) experimental points; (—) sum of calculated profiles.

of the isothermal trace at 203 K shows additionally the contribution at low frequencies of a wide peak which is identified as the tail of the segmental mode of the plasticized wet sample, $\alpha_{w(w)}$. As the temperature increases, similar features are observed together with the displacement of the maxima of the peaks to higher frequencies. At $T > 253$ K the γ_w mode for the wet sample exits the frequency window used in this work. In Figure 4b the isothermal for 273 K is plotted, and the sum of the β_w peak and the tail of the wide $\alpha_{w(w)}$

mode is sufficient to describe the variation of $\epsilon''(\nu)$ down to low frequencies where the contribution of the conductivity has to be included. Additionally, there is another feature observed in Figure 3 which deserves discussion, i.e., the apparent intensity increase of the β_w mode as the temperature reaches 273 K and up to 333 K when it finishes its transit in the frequency window of this work. The observed increase in the intensity of the spectrum is attributed to the presence of a peak insensitive to frequency, detected in the isochrone traces, which in frequency domain is seen as a rise in the background of the loss spectrum. This peak, which temperature of the maximum does not change with frequency, is clearly seen at 288 K in the case of polypropylene/nylon-6 blends²¹ in the wet state where the high-temperature contribution is much less important; it completely disappears as the temperature is decreased from 378 K and reappears with the same characteristics when the sample is hydrated again. This same behavior is observed in the homopolymer. A possible explanation is that this peak corresponds to a phase transition, possibly occurring within the clusters of water molecules existing in the sample.

In Figure 4c corresponding to the isothermal run taken at 353 K, the local modes have swept the entire frequency range, and the loss spectrum can be described by the sum of a very broad $\alpha_{w(w)}$ mode and the appearance of a well-defined $\alpha_{d(w)}$ (α_d of the wet material) peak which is assigned to the segmental mode of the unplasticized material in the wet sample. At still lower frequencies the possible contributions of slower relaxation modes together with the onset of the conductivity have to be taken into account to fit the experimental trace. At 393 K, the coexistence of two segmental relaxations is also observed, and it may be interpreted as the existence of two distinct distributions for the size of the cooperative rearrangement regions (CRR) proposed by Adam and Gibbs²² resulting from the loss of water molecules during the drying process. This interpretation will be further documented after the presentation of the results obtained for the dry sample in the following section. Additionally, at the highest temperature presented in Figure 4d, the introduction of a third intense relaxation mode, α'_w , is necessary to fit the experimental trace. Its origin could be an interfacial polarization due to the semicrystalline character of this polymer, where the size of the relaxing dipoles would justify the high-intensity values recorded for this peak together with the similarity between the activation energy for the mobility of free carriers and the relaxation energy calculated below. In nylon-12 a similar mode has been attributed to long-range displacements by small jumps over potential barriers similar to those overcome in the dc conductivity by ions and protons.¹¹

The final results obtained from the fitting of the isothermal curves recorded by 5 K steps over 9 decades are gathered in the relaxation plot in Figure 5 for the wet nylon-6. The variation of the average relaxation time of the Cole–Cole distributions for each mode as a function of $1000/T$ is represented here. The γ_w and β_w modes originated by the localized motions of small dipolar segments show an extended Arrhenius dependence from which the relaxation parameters, Cole–Cole average activation energies E_{γ_w} and E_{β_w} , and preexponential factors $\tau_{0\gamma_w}$ and $\tau_{0\beta_w}$ can be precisely calculated. The results are reported in Table 1.

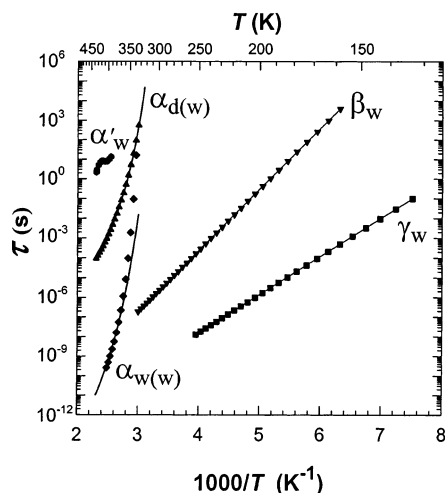


Figure 5. Relaxation plot for the wet nylon-6 sample. Data taken during the increasing temperature run, program A. The lines are the best fit to the data, and the resulting Arrhenius or VTF parameters are reported in Table 1.

Table 1. Relaxation Parameters for the Modes in the Wet and Dry Samples of Nylon-6

	τ_0 (s)	E_A (eV)	τ'_0 (s)	E_{VTF} (eV)	T_0 (K)
Wet Sample					
γ_w mode	3.0×10^{-16}	0.384			
β_w mode	9.0×10^{-17}	0.616			
$\alpha_{d(w)}$ mode	1.9×10^{-9}		1.9×10^{-9}	0.159	263
Dry Sample					
γ_d mode	2.6×10^{-17}	0.477			
β_d mode	1.5×10^{-15}	0.620			
$\alpha_{d(d)}$ mode	1.9×10^{-9}		1.9×10^{-9}	0.159	263

As the temperature increases, the segmental modes appear in the frequency window, first the segmental mode given by the wet sample, $\alpha_{w(w)}$, and then as the sample loses humidity the $\alpha_{d(w)}$ mode corresponding to the dielectric manifestation of the glass transition of the dry nylon-6 in the increasing temperature run; both segmental mobilities correspond to CRR of different sizes. The segmental nature of the $\alpha_{w(w)}$ and $\alpha_{d(w)}$ modes is confirmed by their non-Arrhenius character which is evidenced by the curvature of the $\log(\tau(T))$ data. The relaxation times variation could be fitted to a VTF dependence whose relaxation parameters for the $\alpha_{d(w)}$ mode are reported in Table 1. The VTF parameters of the $\alpha_{d(w)}$ mode in the wet sample are in good agreement with the values obtained by TSDC.² The relaxation time values for the $\alpha_{w(w)}$ mode in the wet sample are strongly affected by the changes that the material is undergoing as the temperature increases due to the reduction of the moisture content as the sample progressively dries. These average relaxation times represented by filled diamond-shaped symbols in Figure 5 correspond to wet materials with different plasticization degrees. If one fits the experimental points in a wide temperature range by taking into account τ values determined from the tails of the modes, VTF parameters are found which are not as reliable as those determined for the $\alpha_{d(w)}$ mode. Even if the VTF energy $E_{VTF} = 0.10$ eV is lower than that found for the $\alpha_{d(w)}$ (see Table 1) which occurs at higher temperature, the value of the T_0 parameter is too high (308 K) as compared to that of the segmental mobility at higher temperatures. Also, the fitting of this peak is strongly affected by the presence of a significant background variable with temperature, which in the frequency domain is the manifestation of the clusters

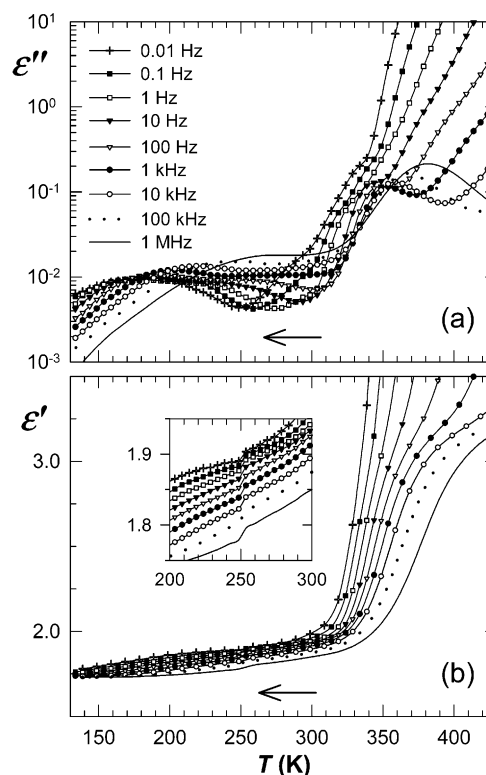


Figure 6. Variation of the imaginary (a) and real (b) part of the dielectric constant of the dry nylon-6 film for frequencies $0.01 \text{ Hz} \leq \nu \leq 3 \text{ MHz}$. Data taken during the cooling run, program A.

of water, which undergo a phase transition in the material.

The α'_w mode is the highest temperature relaxation and the most intense of the spectrum in both states of nylon-6. It is mounted on the steep rise due to the conductivity of the sample. Its presence in the frequency range consists of the high-frequency tail of the peak, and only for temperature higher than 383 K is the maximum observed (see Figure 4d). In Figure 5 the variation of the relaxation times for the α'_w peak is plotted vs $1000/T$ for a short temperature interval. The results do not show a clear trend, and no relaxation parameters were extracted from this short appearance in the relaxation plot. A mode with similar characteristics has been identified in nylon-12,^{11,23} i.e., an intense peak mounted on the high-temperature/low-frequency rise originated by the displacement of free carriers and which is attributed to the conductivity of the sample through long-range diffusion of protons or impurity ions or other kinds of synthesis residuals.

Additional information on the variation with temperature of the dielectric increment, $\Delta\epsilon$, related to the area under the loss curve given by each mode, will be given below when a comparison of these parameters obtained on the wet and dry samples will be performed.

Determination of the Relaxation Time Distribution for Each Mode in the Dry Sample. A similar analysis is carried on for the data obtained in the runs taken from 428 to 133 K, by 5 K steps, each one with a duration of 17 min, that is on the dry sample, and the results of $\log(\epsilon''(T))$ and $\epsilon'(T)$ for frequencies $10^{-2} \text{ Hz} \leq \nu \leq 10^6 \text{ Hz}$ are presented in parts a and b of Figure 6, respectively. In this broad frequency range the results

obtained with a fast temperature ramp at 100 and 1000 Hz (see Figure 1a,b) are confirmed.

In Figure 6a, the results of $\log(\epsilon''(T))$ are plotted over eight frequency decades. The γ_d mode is more intense than in the wet sample and slightly shifted to higher temperatures while the β_d mode is now much weaker than γ_d but has not totally disappeared. The peaks corresponding to the α_w mode are not detected by visual inspection. It will be shown below that there is still a weak contribution of this peak labeled $\alpha_{w(d)}$, found when the detailed analysis is performed on the isothermal loss curves. On the contrary, the high-temperature zone of the spectra given by both states is quite similar; the $\alpha_{d(d)}$ peak, which is now the main glass transition relaxation in the dry sample, is in the same temperature position as the $\alpha_{d(w)}$ in the wet sample with a very slight intensity increase for the dry film.

This is a confirmation of the α_d peak origin attributed to the glass transition temperature of the dry nylon-6 in the runs performed with increasing, $\alpha_{d(w)}$, or decreasing temperature, $\alpha_{d(d)}$. The material is rigidized by the existence of intrachain and interchain H bonds between amide groups which were disrupted by the introduction of water molecules in the wet sample. The results obtained for the variation of $\epsilon'(T)$ are plotted in Figure 6b, where the high-temperature zone corresponds to the glass transition of the dry nylon-6 sample, $\alpha_{d(d)}$. Additionally, there is a step, of very weak amplitude, that is recorded at 253 K and which is amplified in the inset of Figure 6b. This step is not sensitive to the frequency changes, and it is located in the same temperature region as the common rise of the $\epsilon''(T)$ traces recorded in the increasing temperature run (see Figure 3a). In the dielectric absorption plot shown in Figure 6a, it is somewhat difficult to observe this transition as it is mounted on the tail of the higher temperature contributions which are far more intense. The existence of this feature in both heating and cooling runs, which is interpreted as a structural phase transition in a confined environment of clustered water molecules, shows that water exists in all its forms in both states of the material but in different proportions. The amount of water in the sample is now much less than before as deduced from comparison of Figures 3 and 6. Nevertheless, after such a thorough drying procedure, where the sample has been taken to 428 K and kept above 373 K for several hours, the sample is not fully dried.

The information extraction from the DS isothermal experiments is performed as before in the frequency domain by fitting the isothermal $\log(\epsilon''(\nu))$ experimental traces taken every 5 K while the temperatures goes from 428 to 133 K and sweeping at each temperature the chosen frequency range. A sequence of four of these decompositions in Cole–Cole distributions is shown in Figure 7. Figure 7a, corresponding to the 393 K isotherm, is very similar to that shown in Figure 4d for the wet material, the $\alpha_{d(d)}$ being now more intense. The contribution of the $\alpha_{w(d)}$ has to be included in order to fit the experimental trace showing that even after the thermal treatment some plasticization is present in the dry sample. As the temperature decreases, the $\alpha_{w(d)}$ mode sweeps the frequency range as shown in the sequence shown in Figure 7. Also, the conductivity is included at the two highest temperature decompositions presented in Figure 7; at the highest temperatures an intense peak labeled α_w is clearly defined in the peak decomposition as seen in Figure 7a. In the 203 K

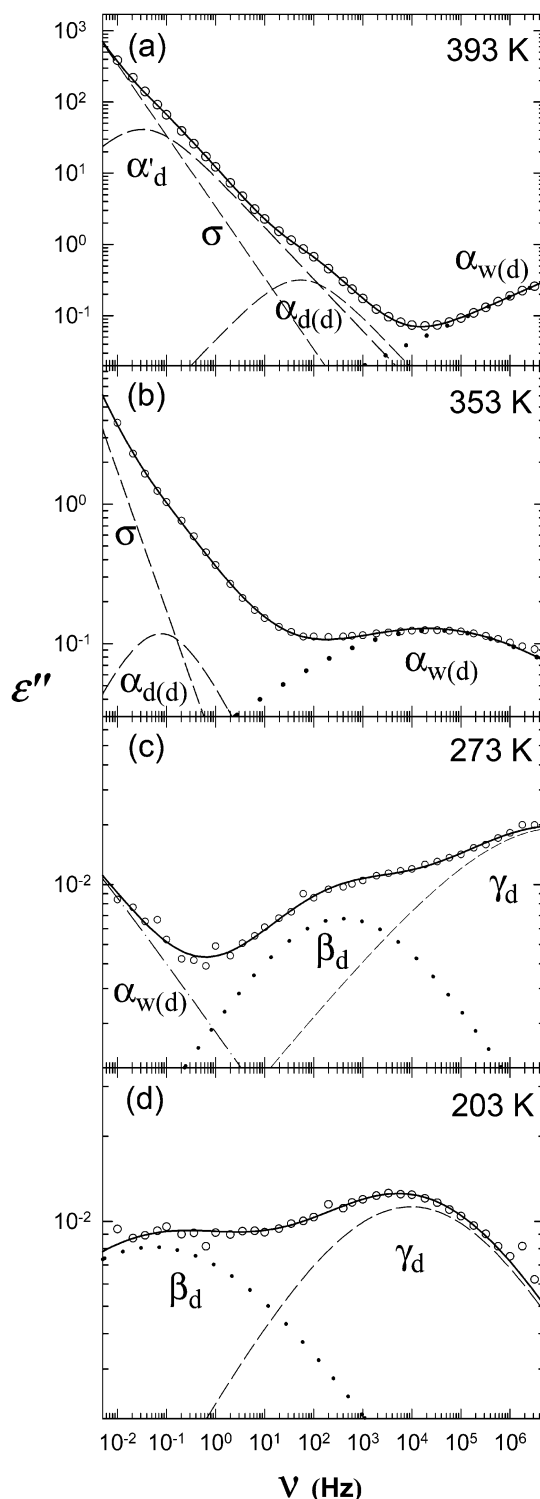


Figure 7. Decomposition in Cole–Cole distributions of the isothermal runs $\epsilon''(\nu)$ for the dry nylon-6 sample: (O) experimental points; (—) sum of calculated profiles.

isotherm, the γ_d and β_d modes are the only ones comprised in our frequency window.

In Figure 8, the comparison of $\epsilon''(\nu)$ at four temperatures is plotted to show the significant differences among the two states of the material and to justify the differences observed in the relaxation plots of both samples. A feature observed in these curves is the inversion in the relative intensities of the γ and β modes for the wet and dry states of nylon-6, together with a shift to lower frequencies for the γ_d mode in dry samples.

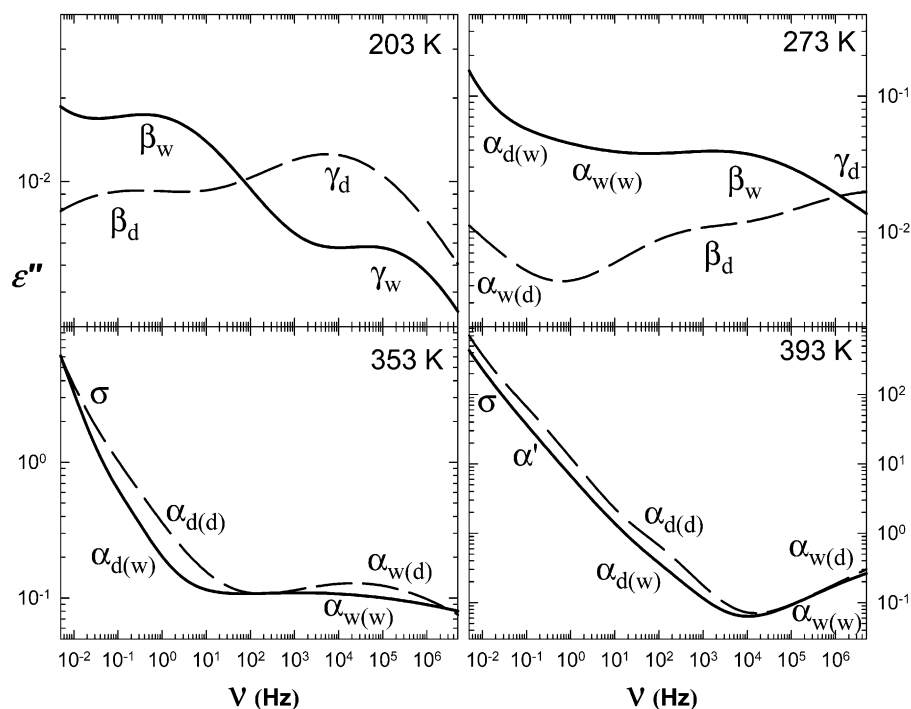


Figure 8. Comparison of the wet (interrupted line) and dry (continuous line) dielectric spectrum for Ny-6.

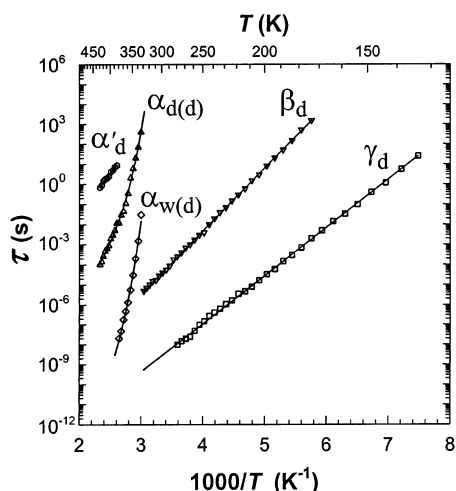


Figure 9. Relaxation plot for the dry nylon-6 sample. Data taken during the cooling run, program A. The lines are the best fit to the data, and the resulting Arrhenius or VTF parameters are reported in Table 1.

When the $\alpha_{d(d)}$ mode is observed, the trace corresponding to the dry sample is slightly more intense, showing that on the increasing temperature run the elimination of the moisture is not complete and that the high-temperature steps in the decreasing temperature run slightly improve the dryness of the sample.

The spectrum decomposition by using Cole–Cole distributions for each peak allows the determination of the relaxation times reported in Table 1 for the dry sample, and in Figure 9 the variation of $\log(\tau)$ as a function of $1000/T$ is plotted for the various modes identified. The γ_d and β_d modes present extended Arrhenius plots that when compared to the relaxation plot in Figure 5 show very little differences in the slope of the linear dependence of the β_d relaxation times and a more important one for the γ_d mode. These differences are quantified in the mean activation energies reported in Table 1 for these modes. The γ activation energy goes

from 0.384 to 0.477 eV whereas the β one is almost constant varying from 0.616 to 0.620 eV on going from the wet to the dry state. These values for the γ modes agree very well with those reported previously for nylon-6,6 by Starkweather and Barkley,²⁴ who found a variation of the γ activation energy $0.39 \text{ eV} \leq E_\gamma \leq 0.48 \text{ eV}$ on going from the wet to the dry film. The relaxation times calculated by Pathmanathan et al.¹⁸ for nylon-12 from the variation of the position of the maxima of the dielectric loss peaks show significantly lower energies than those found here for nylon-6, 0.25–0.29 eV, as the water content decreases. This could be related to the number of amide groups per 100 chain atoms, which is 7.7 in nylon-12; the number in nylon-6 and nylon-6,6 is twice as much. This difference in the number of H bonds between amide groups may account for the variation in the reorientation energies of the local motions involving the shortest chain segments which are at the origin of the lowest temperature modes in nylon-6. For the β mode the results differ between nylon-6 and nylon-6,6 as the activation energy in our case is almost constant (from 0.616 to 0.620 eV), and in the latter one the reported variation is from 0.57 to 0.91 eV²⁴ as less water is present. Our TSDC results on nylon-6 show² that the β mode position of maximum is independent of the hydration level, and thus its activation energy was found constant as it is the case in the dielectric spectroscopy determination presented here. The wide variation range reported on nylon-6,6 might be due to the overlap of the β mode and the segmental relaxation which made the resolution difficult in the restricted frequency and temperature ranges used.

As for the segmental relaxations corresponding to the dry nylon-6, $\alpha_{d(w)}$ and $\alpha_{d(d)}$, the relaxation times determined as a function of temperature, for either the wet or the dry samples, show a VTF behavior which parameters are identical, showing that the effect of a more thorough drying procedure does not affect the segmental mobility reached in the heating run. These parameters define a cooperative mobility which characterize the

most dry state that can be reached with this kind of thermal treatment. At lower temperatures, the α_w mode of the dry sample, labeled here for clarity $\alpha_{w(d)}$, obeys a non-Arrhenius dependence as shown in Figure 9. An acceptable fit to a VTF curve can be reached, but the values of the parameters as in the case of the $\alpha_{w(w)}$ are not reliable ($E_{VTF} = 0.13$ eV, $T_0 = 284$ K) as the material is still changing because of the effect of the variations in the state of the humidity still trapped in the film. Even though the VTF energies as compared to those determined for the dry state are lower, the T_0 value is too large for a mode located at lower temperatures than the $\alpha_{d(d)}$. The two wet states found during the increasing and decreasing temperature runs show relaxation times that are lower for the driest film seeming to indicate an unexpected change in the plasticization of the sample.

The coexistence of two segmental mobilities found in this work in nylon-6 is not interpreted as an amorphous T_g or $T_g(l)$ and a separate crystalline-dominated T_g or $T_g(u)$ proposed by Rotter and Ishida,⁶ the latter one associated with the presence of tie molecules, loose loops, and cilia existing in the amorphous phase located at the interfaces. Their interpretation is sustained on the results on samples with various crystallinity degrees; this parameter is not changing in our experiments. Besides, the energies reported in the DMA work are far too high as expected when using Arrhenius dependences. The coexistence of two T_g reported in our work seems to agree better with a representation of different spatial scales, i.e., smaller CRR sizes corresponding to faster modes, α_w , and larger CRR giving rise to slower ones, α_d . A second or additional glass transition has been found in the mixed alkali effect in inorganic glasses and attributed to disconnected CRR of high mobility and connected regions of lower mobility.²⁵ In the case of poly(*n*-alkyl methacrylates) Beiner et al.²⁶ have also found the coexistence of two glass transitions. Two alternative pictures are drawn in their work to interpret the coexistence of two segmental modes in these homopolymers. The static picture is based on a nanophase separation which is analogous to the microphase separation in block copolymers but on a shorter length scale. The dynamic picture appeals to the existence of a dynamic heterogeneity whose fluctuation occurs with two characteristic times and length scales. Each part of the poly(*n*-alkyl methacrylate) molecule would participate in two cooperative motions with different time scales. These ideas can be applied in our case where the α_d mode which is independent of the drying procedure duration would be the general glass transition corresponding to the lowest humidity concentration while the lower temperature α_w mode is the additional glass transition which varies with the amount of humidity in the sample. As in the case of the inorganic glasses with two sorts of alkali ions and the poly(*n*-alkyl methacrylates), the presence of more than one T_g may be attributed here either to a dynamic heterogeneity or to a structural one. In the case of Ny-6 the existence of a nanophase separation seems less probable than in the poly(*n*-alkyl methacrylates) where long alkyl side chains exist; thus, the dynamic picture is more plausible and interesting as a new insight into the dynamic glass transition. This effect should also be present in plasticized polymeric materials which can be visualized as composed of CRR sizes that correspond to sufficiently distinct mobilities.

As for the α'_d mode equivalent to the α'_w peak which was present in the run at increasing temperatures, it is also a wide peak, visible only in the high-temperature isotherms recorded for the dry sample. It is of comparable intensity to the α'_w peak, but in this case a trend can be deduced from the relaxation plot. Its behavior is Arrhenius, and the activation energy is $E_{A\alpha'_d} = 0.87$ eV with a preexponential factor $\tau_0 = 4.5 \times 10^{-11}$ s. This high activation energy and temperature dependence are compatible either with a relaxation originated by the motion of the chains in the lamellae which has been found in poly(vinylidene fluoride) (PVDF)¹⁶ and polyethylene²⁷ or with the diffusion of carriers such as protons and other defects, i.e., a mechanism related to the existence of large dipoles possibly due to the accumulation of charges at the interfaces. In PVDF the Arrhenius activation energy of the α_c mode was found equal to 0.49 eV, but higher values had also been reported. Moreover, the intensity of the α_c mode in PVDF is less intense than the segmental mode, which is not the case here. These characteristics seem to agree with the proposition¹² that this kind of chain motions in polyamides should not exist due to the amplitude of the displacements involved and to the existence of interchains H bonds. The high activation energy and intensity found here point to a Maxwell–Wagner–Sillars (MWS) relaxation, in agreement with Steeman and Maurer,²⁸ on nylon-4,6 and nylon-6,6. This mode is highly related to the mobility of free carriers as proposed by Eley et al. in biopolymers²⁹ and also in agreement with the interpretation for the α' peak in nylon-12.^{11,23} Electrical conductivity and dielectric studies in nylon-11³⁰ showed that space charge polarization and MWS effects are negligible in that polyamide as the high ϵ'' at low frequencies are not accompanied by high ϵ' values. This is not observed in our case as the low-frequency values of ϵ' at high-temperature surpass 10^3 in both the wet and dry samples. Studies on polypropylene/nylon-6 blends, where the crystallinity could be widely varied by functionalizing the polypropylene, show that the α' mode disappears in the nearly amorphous blends.²¹ The role of the crystalline lamellae at the origin of this peak is thus proved, and the possibility of attributing this high-temperature mode to an interfacial relaxation due to the presence of crystalline regions will justify the high activation energy value related to the migration energy of charges trapped at the interfaces.

Another quantity that is extracted from the decomposition of $\epsilon''(\nu)$ in Cole–Cole distributions is the dielectric increment, $\Delta\epsilon_{C-C}$, evaluated at each temperature from the area under the curve of each mode in frequency domain. This quantity, which is proportional to the number of reorienting dipoles times the square value of the effective dipolar moment originating the relaxation mode, is plotted for each mode in Figure 10 as a function of temperature. Figure 10a shows that the β mode is the most intense of the local modes in the wet sample where a very low contribution from the γ mode is also observed. Opposite results are calculated for the dry sample in Figure 10b where the γ relaxation predominates at low temperatures. Both local modes present a wide relaxation time distribution as characterized by the α Cole–Cole parameter comprised between 0.2 and 0.4 for both sample hydration states.

The results for the segmental modes are about 10 times more intense than those of the local modes as seen in parts c and d of Figure 10 for the wet and dry

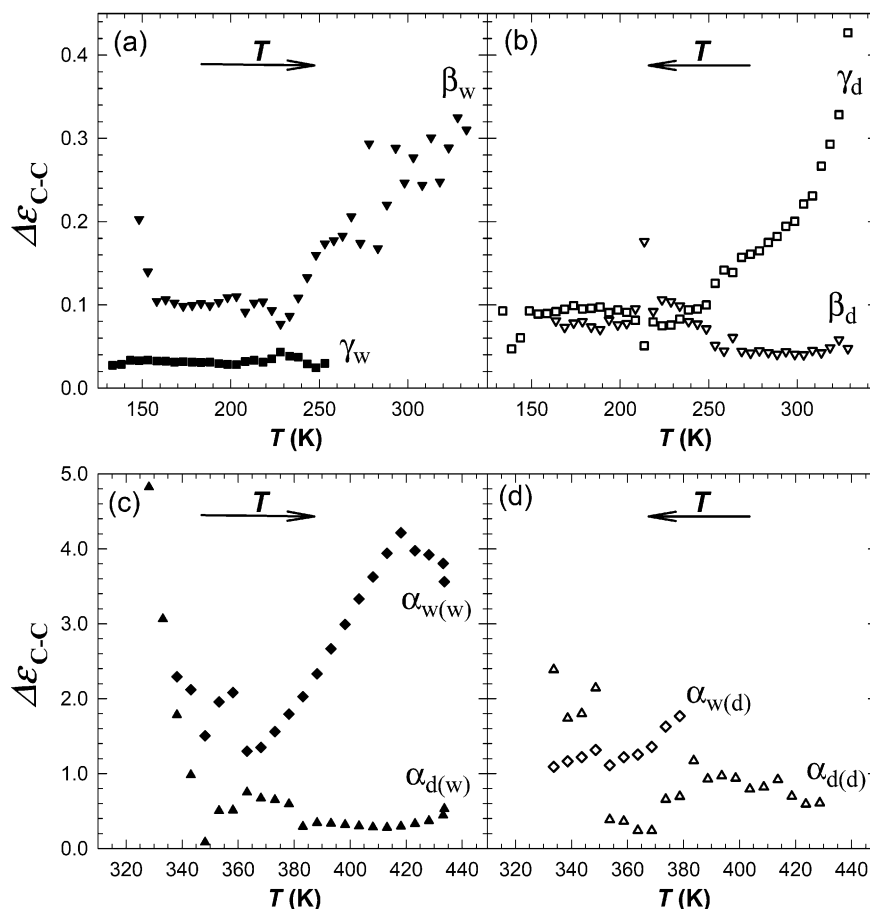


Figure 10. Dielectric increment from Cole–Cole distribution parameters for the wet and dry samples of nylon-6: (a) γ_w and β_w modes for the wet sample; (b) γ_d and β_d modes for the dry sample; (c) $\alpha_{w(w)}$ and $\alpha_{d(w)}$ for the wet sample; (d) $\alpha_{w(d)}$ and $\alpha_{d(d)}$ for the dry sample.

samples, respectively. In the wet sample the dielectric increment is about 4 times larger for the $\alpha_{w(w)}$ than for the $\alpha_{w(d)}$, showing the plasticization effect of water. The decrease observed in the $\alpha_{d(w)}$ intensity is the expected behavior for a cooperative mode.³¹ For the $\alpha_{w(w)}$ mode the complex behavior found for the $\Delta\epsilon_{C-C}$ results from the effect of the variation of the background as the temperature and the effectivity of the drying procedure increase. This behavior evidences that the parameters found for the $\alpha_{w(w)}$ mode do not correspond to the same segmental mode.

Conclusions

The experimental results on nylon-6 reported here show several new results and confirm known features observed on this important polymer in a more quantitative form due to the precise determination of the relaxation times variation with temperature performed in a broad frequency and temperature range. The results reported here evidence the existence of two local modes which relative contributions depend on the water content of the sample, two segmental modes attributed to the wet and dry material, a MWS relaxation at high temperatures and low frequencies, and a significant contribution of the dc conductivity observed as a steep increase at low frequencies and high temperatures. The differences observed in the runs performed as the temperature increases evidenced changes in the material where water desorbs as the temperature rises although the film is clamped between capacitor metallic plates. Similar experiments on nylon-4,6 and -6,6 led

to the conclusions that because of the clamping and of the dry nitrogen flow water desorption was strongly hindered,²⁸ which is not true in our work.

The observation of two segmental relaxations due to two different scales of cooperative motions, reflected in the sizes of the CRR regions and in the two different time ranges, is proposed here as the explanation for the coexistence of the $\alpha_{w(w)}$ and $\alpha_{d(w)}$ relaxation modes in the wet material. The decrease in the $\alpha_{w(d)}$ mode together with the predominance of the γ over the β mode observed during the decreasing temperature run confirms the desorption of water molecules in the measuring cell.

As for the relaxation parameters calculated from the relaxation times variation with temperature, the segmental character of the α_w and α_d modes in the two humidity states studied here is confirmed by the VTF dependence found in a wide temperature and frequency range. The identical parameters found for the α_d for both the dry and wet films indicate the dry state reached is stable and characteristic of the nylon-6 but does not correspond to an absence of water molecules in the polymer. Referring to the local modes, the β activation energy is less sensitive than that of the γ mode to the water content, as the values found for the wet and dry samples differ by less than 1%; for nylon-12⁵ and nylon-6,^{6,24} as the sample desorbs water the Arrhenius β energy increases more significantly, except for nylon-4,6 where it is proposed that the interchains H bond are weakened by the presence of water molecules.²⁸

Additionally, it is a general characteristic that the Cole–Cole distributions are wide for the local relaxation modes found for both the wet and the dry samples, with low values varying between 0.2 and 0.4 for the α Cole–Cole width parameter, showing that the local energy landscape for the reorientations responsible for the local modes, i.e., rotation of amide groups, vary widely through the material. Also, the width parameters found for the $\alpha_{d(w)}$ and $\alpha_{d(d)}$ modes are closer to one than those found for the $\alpha_{w(w)}$ and $\alpha_{w(d)}$ modes, which vary between 0.2 and 0.4, showing that the cooperativity in the dry case develops in a more homogeneous environment.

Acknowledgment. We thank Dr. M. A. Gomez for kindly supplying the nylon-6 films used here. This work is part of Project G97-000594, FONACIT, and we thank them for their financial support.

References and Notes

- (1) Frank, B.; Frubing, P.; Pissis, P. *J. Polym. Sci., Part B: Polym. Phys.* **1996**, *34*, 1853.
- (2) Laredo, E.; Hernández, M. C. *J. Polym. Sci., Part B: Polym. Phys.* **1997**, *35*, 2879.
- (3) Puffr, R.; Sebenda, J. *J. Polym. Sci., Part C* **1967**, *16*, 79.
- (4) Rong, S.; Williams, H. L. *J. Appl. Polym. Sci.* **1985**, *30*, 2575.
- (5) Varlet, J.; Cavallé, J. Y.; Perez, J.; Johari, G. P. *J. Polym. Sci., Part B: Polym. Phys.* **1990**, *28*, 2691.
- (6) Rotter, G.; Ishida, H. *Macromolecules* **1992**, *25*, 2170.
- (7) Boyd, R. H. *J. Chem. Phys.* **1959**, *30*, 1276.
- (8) McCrum, N. G.; Read, B. E.; Williams, G. *Anelastic and Dielectric Effects in Polymeric Solids*; Dover: New York, 1991; p 478.
- (9) Yemni, T.; Boyd, R. H. *J. Polym. Sci., Polym. Phys.* **1979**, *17*, 741.
- (10) Yemni, T.; Boyd, R. H. *J. Polym. Sci., Polym. Phys.* **1976**, *14*, 499.
- (11) Pathmanathan, K.; Johari, G. P. *J. Chem. Soc., Faraday Trans.* **1995**, *91*, 337.
- (12) Boyd, R. H. *Polymer* **1985**, *26*, 1123.
- (13) Avakian, P.; Matheson, R. R., Jr.; Starkweather, H. W., Jr. *Macromolecules* **1991**, *24*, 4698.
- (14) Campoy, I.; Arribas, J. M.; Zaporta, M. A. M.; Marco, C.; Gomez, M. A.; Fatou, J. G. *Eur. Polym. J.* **1995**, *1*, 475.
- (15) Grima, M.; Laredo, E.; Perez, M. C.; Bello, A. *J. Chem. Phys.* **2001**, *114*, 6417.
- (16) Bello, A.; Laredo, E.; Grima, M. *Phys. Rev. B* **1999**, *60*, 12764.
- (17) Garwe, F.; Schönhals, A.; Lockwenz, H.; Beiner, M.; Schröter, K.; Donth, E. *Macromolecules* **1996**, *29*, 247.
- (18) Pathmanathan, K.; Cavallé, J. Y.; Johari, G. P. *J. Polym. Sci., Part B: Polym. Phys.* **1992**, *30*, 341.
- (19) Massalska-Arodz, M.; Williams, G.; Thomas, D. K.; Jones, W. J.; Dabrowski, R. *J. Phys. Chem. B* **1999**, *103*, 4197.
- (20) Massalska-Arodz, M.; Williams, G.; Smith, I. K.; Conolly, C.; Aldridge, G. A.; Dabrowski, R. *J. Chem. Soc., Faraday Trans.* **1998**, *94*, 387.
- (21) Grima, M.; et al. To be published.
- (22) Adam, G.; Gibbs, J. H. *J. Chem. Phys.* **1965**, *43*, 139.
- (23) Pathmanathan, K.; Johari, G. P. *J. Polym. Sci., Part B: Polym. Phys.* **1993**, *31*, 265.
- (24) Starkweather, H. W., Jr.; Barkley, J. R. *J. Polym. Sci., Polym. Phys. Ed.* **1981**, *19*, 1211.
- (25) Donth, E. In *The Glass Transition Relaxation Dynamics in Liquids and Disordered Materials*; Springer-Verlag: Berlin, 2001; p 170.
- (26) Beiner, M.; Schröter, K.; Hempel, E.; Reissig, S.; Donth, E. *Macromolecules* **1999**, *32*, 6278.
- (27) Graff, M. S.; Boyd, R. H. *Polymer* **1994**, *35*, 1797.
- (28) Steeman, P. A. M.; Maurer, F. H. J. *Polymer* **1992**, *33*, 4236.
- (29) Eley, D. D.; Lockhart, N. C.; Richardson, C. N. *J. Chem. Soc., Faraday Trans. 1* **1979**, *75*, 323.
- (30) Neagu, M. R.; Neagu, E.; Bonanos, N.; Pissis P. *J. Appl. Phys.* **2000**, *88*, 6669.
- (31) Schönhals, A. In *Dielectric Spectroscopy of Polymeric Materials*; Runt, J. P., Fitzgerald, J. J., Eds.; American Chemical Society: Washington, DC, 1997; p 81.

MA034954W